

Status of the diagnostics development for the first operation phase of the stellarator Wendelstein 7-Xa)

R. König, W. Biel, C. Biedermann, R. Burhenn, G. Cseh, A. Czarnecka, M. Endler, T. Estrada, O. Grulke, D. Hathiramani, M. Hirsch, S. Jabłonski, M. Jakubowski, J. Kaczmarczyk, W. Kasperek, G. Kocsis, P. Kornejew, A. Krämer-Flecken, M. Krychowiak, M. Kubkowska, A. Langenberg, M. Laux, Y. Liang, A. Lorenz, O. Neubauer, M. Otte, N. Pablant, E. Pasch, T. S. Pedersen, O. Schmitz, W. Schneider, H. Schuhmacher, B. Schweer, H. Thomsen, T. Szepesi, B. Wiegel, T. Windisch, S. Wolf, D. Zhang, and S. Zoletnik

Citation: [Review of Scientific Instruments](#) **85**, 11D818 (2014); doi: 10.1063/1.4889905

View online: <http://dx.doi.org/10.1063/1.4889905>

View Table of Contents: <http://scitation.aip.org/content/aip/journal/rsi/85/11?ver=pdfcov>

Published by the [AIP Publishing](#)

Articles you may be interested in

[Diagnostics development for quasi-steady-state operation of the Wendelstein 7-X stellarator \(invited\)a\)](#)

Rev. Sci. Instrum. **83**, 10D730 (2012); 10.1063/1.4733531

[Diagnostic developments for quasicontinuous operation of the Wendelstein 7-X stellaratora\)](#)

Rev. Sci. Instrum. **79**, 10F337 (2008); 10.1063/1.2964998

[Bayesian experimental design of a multichannel interferometer for Wendelstein 7-Xa\)](#)

Rev. Sci. Instrum. **79**, 10E712 (2008); 10.1063/1.2956962


[Energetic ion loss diagnostic for the Wendelstein 7-AS stellarator](#)

Rev. Sci. Instrum. **72**, 2936 (2001); 10.1063/1.1379602


[Proposed neutron diagnostics for Wendelstein 7-X stellarator](#)

Rev. Sci. Instrum. **70**, 1185 (1999); 10.1063/1.1149321


Frustrated by old technology?



Is your AFM dead and can't be repaired?



Sick of bad customer support?



It is time to upgrade your AFM

Minimum \$20,000 trade-in discount for purchases before August 31st

Asylum Research is today's technology leader in AFM

dropmyoldAFM@oxinst.com

OXFORD
INSTRUMENTS

The Business of Science®

Status of the diagnostics development for the first operation phase of the stellarator Wendelstein 7-X^{a)}

R. König,^{1,b)} W. Biel,² C. Biedermann,¹ R. Burhenn,¹ G. Cseh,³ A. Czarnecka,⁴ M. Endler,¹ T. Estrada,⁵ O. Grulke,¹ D. Hathiramani,¹ M. Hirsch,¹ S. Jablonski,⁴ M. Jakubowski,¹ J. Kaczmarczyk,⁴ W. Kasperek,⁶ G. Kocsis,³ P. Kornejew,¹ A. Krämer-Flecken,² M. Krychowiak,¹ M. Kubkowska,⁴ A. Langenberg,¹ M. Laux,¹ Y. Liang,² A. Lorenz,¹ O. Neubauer,² M. Otte,¹ N. Pablant,⁷ E. Pasch,¹ T. S. Pedersen,¹ O. Schmitz,⁸ W. Schneider,¹ H. Schuhmacher,⁹ B. Schweer,² H. Thomsen,¹ T. Szepesi,³ B. Wiegel,⁹ T. Windisch,¹ S. Wolf,⁶ D. Zhang,¹ and S. Zoletnik³

¹Max Planck Institute for Plasma Physics, 17491 Greifswald, Germany

²Institute of Energy and Climate Research, Forschungszentrum Jülich GmbH, D-52425 Jülich, Germany

³Wigner RCP, RMI, Konkoly Thege 219–33, H-1121 Budapest, Hungary

⁴IFPiLM, Hery Street 23, 01–497 Warsaw, Poland

⁵Laboratorio Nacional de Fusion, CIEMAT, Avenida Complutense, Madrid, Spain

⁶IGVP, Universität Stuttgart, Pfaffenwaldring 31, 70569 Stuttgart, Germany

⁷Princeton Plasma Physics Laboratory, Princeton, New Jersey 08543, USA

⁸Department of Engineering Physics, University of Wisconsin–Madison, 1500 Engineering Drive, Madison, Wisconsin 53706, USA

⁹Physikalisch-Technische Bundesanstalt, Bundesallee 100, 38116 Braunschweig, Germany

(Presented 3 June 2014; received 29 May 2014; accepted 25 June 2014; published online 18 July 2014)

An overview of the diagnostics which are essential for the first operational phase of Wendelstein 7-X and the set of diagnostics expected to be ready for operation at this time are presented. The ongoing investigations of how to cope with high levels of stray Electron Cyclotron Resonance Heating (ECRH) radiation in the ultraviolet (UV)/visible/infrared (IR) optical diagnostics are described. [<http://dx.doi.org/10.1063/1.4889905>]

I. INTRODUCTION

The commissioning phase of the superconducting stellarator Wendelstein 7-X (W7-X)^{1,2} (Fig. 1) has just started and the first plasma operation phase (OP1.1) of 3 months duration is expected to begin in about a year's time. At the start of this period all in-vessel components will already be installed, except for the uncooled divertor, the heat shield like baffle structure and the carbon tiles not yet being attached onto the heat shields. These missing components will only be available for the 2nd part of the first operation phase OP1.2. In OP1.1 five uncooled inboard poloidal fine corn graphite limiters, suitably shaped to match a specially selected limiter configuration, will insure the protection of all in-vessel components. The OP1.1 phase will allow an early commissioning and demonstration of the operation of the control and safety systems for the W7-X device components, like vacuum system, cryogenics, magnetic field coils, and Electron Cyclotron Resonance Heating (ECRH). Moreover, most of the diagnostics will be commissioned and tested for OP1.2 (expected to start in summer 2016), albeit them not yet being fully integrated into the standard W7-X data acquisition and control system at this time. Assuming the heat loads can be spread out evenly across the limiters, e.g., 1 s discharges at 2 MW

of heating power (ECRH) could be achieved. These pulse parameters will be sufficient to demonstrate the readiness of the installed diagnostics and even to run a first physics program,² albeit restricted to limiter configurations only.

II. DIAGNOSTICS FOR OP1.1

A. Essential diagnostics

A set of 8 diagnostics has been defined as essential for OP1.1 (Table I): The neutron counters are required to obtain the operation license for W7-X. They will be calibrated just before closing the plasma vessel (early 2015), using an in-vessel railway to transport the ²⁴¹Am/Be calibration source.³ Flux surface measurements (Fig. 2) will be taken from the moment we start energising the superconducting coils, in order to learn how to correct any residual error fields with the trim coils and to gather information how to correct for the effects resulting from the deformation of the coils with increasing field strengths. At the end of OP1.1 it is foreseen to remove the limiters, so that, with the divertors not yet installed, this will give the unique opportunity to investigate the edge magnetic island structures which are essential for divertor operation. The l.o.s. averaged electron density will be provided by a single channel dispersion interferometer (Fig. 3) with an Field Programmable Gate Array (FPGA) based data analysis. We aim at demonstrating the real time capabilities of this system, but without the gas feedback loop yet being implemented. The electron temperature will be provided by a 16 channel Electron Cyclotron Emission (ECE) system, with an

^{a)}Contributed paper, published as part of the Proceedings of the 20th Topical Conference on High-Temperature Plasma Diagnostics, Atlanta, Georgia, USA, June 2014.

^{b)}Author to whom correspondence should be addressed. Electronic mail: rlk@ipp.mpg.de.



FIG. 1. Present status of W7-X construction. The staircase on the left, the attached bridge, which carries the Thomson scattering observation optics and a central bridge support tower along which the Thomson laser beam is guided, ensure that none of the Thomson components is connected to the W7-X device.

additional set of 16 zoom channels. The limiters are equipped with thermo-couples to ensure that the temperature of the support structure does not exceed a critical value in a sequence of pulses. One of the limiters will be equipped with Langmuir probes as well. Ten simplified (not long pulse compatible) IR/visible divertor observation systems will be used to monitor the limiter loads. These systems will be equipped with 10 Near Infrared (NIR) ($\lambda \sim 1 \mu\text{m}$) and 10 visible cameras fitted with various interference filters ($\text{H}\alpha$, $\text{H}\beta$, He II, C II, C III). For OP1.2 two of the 10 systems will be replaced by long pulse compatible endoscopes presently being developed by Thales-SESO. In the remaining 8 simplified systems the NIR cameras will be replaced by 1024×1024 pixel μ -bolometer cameras. The tender for these magnetic field hardened cameras has just been launched. Both systems are covering the entire divertor ($\sim 115^\circ \times 60^\circ$ viewing angle) and are expected to reach a resolution of 6 mm at the low iota end of the divertor and ≤ 10 mm at the far end of the divertor.

B. Diagnostics expected to be ready for OP1.1

A significant number of further diagnostics are expected (though not fully guaranteed) to be available for first operation in OP1.1 (Table I).

Thomson scattering (Fig. 3), pulse height analysis (PHA), density profile reflectometry, poloidal correlation

TABLE I. Diagnostics for OP1.1: 1st set will for sure be installed. Some diagnostics of 2nd set run risk of not getting installed.

Essential diagnostics	Expected diagnostics
Neutron counters	Thomson scattering
Flux surface measurements	HEXOS (VUV spectr.)
Dispersion interferometer	Vertical bolometer camera
Video diagnostic (tor. view)	Therm. He-beam
Electron cyclotron emission	Diamagnetic loops
Limiter diagnostics	Rogowski coil systems
-Thermo-couples in limiter support structure	Neutral pressure gauges
-Limiter Langmuir probes	X-ray imaging system
-2D Infrared/vis. limiter obs.	US X-ray crystal spectr.
	Reflectometry systems
	Pulse height analysis (PHA)
	Z_{eff} Bremsstrahlung

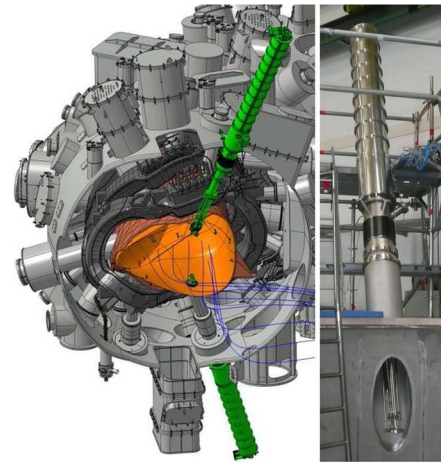


FIG. 2. (Left) Two of the three flux surface measurement systems which each are equipped with a fluorescent rod with an e-gun at its tip. By being fully retractable behind a water cooled, ECRH stray radiation tight port shutter, the systems can be used at any day after the end of plasma operation, even in the later quasi-continuous operation phase of W7-X. (Right) Complete system being set up for operation test in a large vacuum test chamber.

reflectometry, and a new steering Doppler reflectometry system⁴ will provide electron temperatures and densities, while the information on the ion temperatures and impurities will be provided by two X-ray imaging systems, the High Efficiency Extreme Ultraviolet Overview Spectrometer (HEXOS) system⁵ (which has already been operated at TEXTOR with a W7-X Mini-CoDaC system and has meanwhile been installed in its final position at W7-X), at least one of two bolometer cameras and a single i.o.s. visible Bremsstrahlung Z_{eff} observation system. The complete set of magnetics consisting of 3 diamagnetic loops, 3 continuous and 2 segmented Rogowski coils, 20 saddle coils and 124 distributed Mirnov coils, have already been fully installed inside the plasma vessel. For the latter two coil systems, the data acquisition may not yet be available in time for OP1.1. Of the 24 neutral pressure gauges initially only the 5 in the torus midplane will be installed. The head of the midplane multi-purpose manipulator (Fig. 4) will initially be equipped with Langmuir probes, magnetic sensors, and a piezo controlled impurity gas inlet. Two 5-nozzles thermal He-beam gas injection boxes will pri-

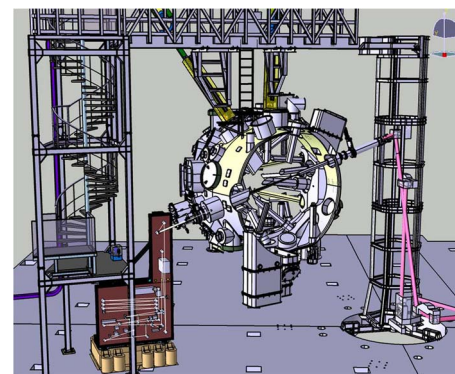


FIG. 3. Thomson bridge with support structure holding underneath the two observation optics and in pink the automatically steered Thomson laser beam. The brown system shows the single channel dispersion interferometer whose laser beam runs collinear to the Thomson beam (allowing easy cross calibration between the two systems).

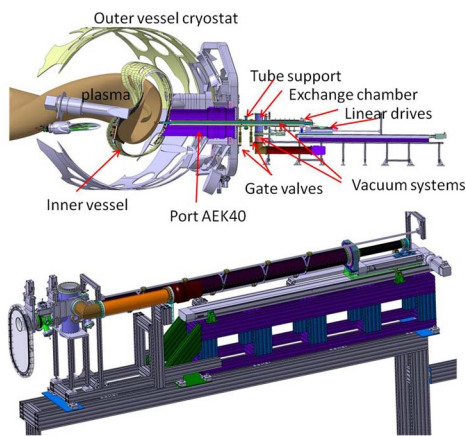


FIG. 4. Torus midplane multi-purpose manipulator which can be equipped with various probe heads.

marily be used for helium gas fuelling in OP1.1, but also first He-beam spectra will be observed via a window attached to a port lid. The actual He-beam observation and visible divertor spectroscopy systems, consisting of 2 sets of two scanning endoscopes, looking almost tangentially and perpendicular onto the target surface at one upper and one lower divertor at the location where the He-beams are integrated into the divertor target plate will be only available for OP1.2. To investigate the ECRH stray radiation distribution in W7-X, 5 sniffer probes at 5 toroidal locations in the W7-X midplane will be used.

III. COPING WITH ECRH STRAY RADIATION IN UV, VISIBLE AND IR SENSITIVE OPTICAL DIAGNOSTICS

One possibility to protect optical diagnostics from being affected by high levels of ECRH stray radiation is to use suitable metal meshes, if required in combination with a special ECRH absorbing $\text{Al}_2\text{O}_3/\text{TiO}_2$ coating on surrounding surfaces, as in case of the W7-X bolometer systems.^{6,7} However, in high spatially resolving systems, in particular in high resolution UV/visible/IR imaging camera systems, the stray light on the grid structure can severely limit the achievable spatial resolution. For the visible spectral range we have demonstrated that the transparent conductive coating ITO (indium tin oxide) applied to an optical window can be used to sufficiently reduce the ECRH transmission (1.2 μm ITO layer: $T_{\text{ECRH}} < 0.5\%$ with T_{vis} between 60% and 90% for λ between 420 nm and 1.4 μm).⁸ Extension of the spectral range into the UV may be possible.⁹

A. Single-wall carbon nanotube (SW-CNT) coating

Hu *et al.*¹⁰ have shown that with single-wall carbon nanotube (SW-CNT) coatings it should be possible to achieve transmission coefficients of $T > 50\%$ for $\lambda > 200$ nm and $T > 90\%$ for $2\mu\text{m} < \lambda < 13\mu\text{m}$ while at the same time reducing the 140 GHz ($\lambda = 2$ mm) ECRH stray radiation transmission by about two orders of magnitude. As a first test the IWS Fraunhofer Institute, Dresden (Germany), prepared sample windows using commercially available SW-CNTs from Nanolab and from IWS Fraunhofer itself. The electrical conductivity of the SW-CNT layers made from Fraunhofer CNTs

were found to be 10–80 times higher, varying with surface density, than those based on Nanolab CNTs. Testing the better suited SW-CNTs made by Fraunhofer in our ECRH lab showed that a surface density of 3 g/m² would be required to limit the ECRH transmission at 140 GHz to less than 1.5%. The corresponding sheet thickness would be 2.2 μm and the resistivity about 3–5 Ω/sq . For these values the IR transmission at $\lambda = 2.5\mu\text{m}$ would be 3.5% and at 3–5 μm only 1.5%. Hu *et al.*¹⁰ achieved a 60 times higher IR transmission at a layer thickness of only 25 nm, a resistivity of 200 Ω/sq and an ECRH transmission $T_{\text{ECRH}} < 1.5\%$. Obviously, the SW-CNT “quality” is extremely important and requires further investigation.

B. IR/visible long pulse compatible divertor observation endoscopes

For the IR/vis. endoscope system the effect of the ECRH stray radiation on the IR detector has been estimated. The optical system has a small 6 mm diameter entrance pupil (pinhole), followed by an aspheric and a planar mirror guiding the radiation to an off-axis Cassegrain system which reflects the radiation to outside the vacuum barrier, where a lens system forms an image of the divertor on a 3–5 μm IR camera. Of the expected 100 kW/m² ECRH stray radiation about 3 W will penetrate through the pinhole, of which $\sim 50\%$ will be absorbed at $\text{Al}_2\text{O}_3/\text{TiO}_2$ absorber coated apertures and tube sections. The other half will be reflected by the metal mirrors and transported through the vacuum window. Behind the intermediate image formed by the last metal mirror, the ECRH radiation diverges, since the following imaging lenses have no focussing effect at this wavelength. Due to the geometry of the setup, this results in a reduction of the ECRH stray radiation at the detector by a factor of 120. An additional $\sim 20\%$ absorption can be expected within the lens system (loss tangent values at 140 GHz have been reported by various authors for many UV/vis./IR optical materials^{11–13}). The remaining ECRH stray radiation at the detector amounts to ~ 10 mW distributed over 1280×1024 pixels or 0.007 $\mu\text{W}/\text{pixel}$. This would correspond to a temperature increase at a pixel of the order of $\Delta T \approx 0.004$ K/s (if fully absorbed), which is well within the cooling capability of the Stirling cooler attached to the sensor.

¹T. Klinger *et al.*, *Fus. Eng. Design* **88**, 461 (2013).

²S. Bosch *et al.*, *IEEE Trans. Plasma Science* **42**, 432 (2014).

³W. Schneider *et al.*, *J. Instrum.* **7**, C03025 (2012).

⁴P. Rohmann *et al.*, in *Proceedings of the IEEE International Symposium on Phased Array Systems and Technology* (IEEE, 2013), p. 559.

⁵W. Biel *et al.*, *Rev. Sci. Instrum.* **77**, 10F305 (2006).

⁶D. Zhang *et al.*, *Rev. Sci. Instrum.* **81**, 10E134 (2010).

⁷R. König *et al.*, *Rev. Sci. Instrum.* **83**, 10D730 (2012).

⁸R. König *et al.*, *Rev. Sci. Instrum.* **81**, 10E133 (2010).

⁹S. Ray, R. Banerjee, N. Basu, A. K. Batabyal, and A. K. Barua, *J. Appl. Phys.* **54**, 3497 (1983).

¹⁰L. Hu *et al.*, *Appl. Phys. Lett.* **94**, 081103 (2009).

¹¹J. W. Lamb, “Miscellaneous data on materials for mm- and sub-mm optics,” *Int. J. Infrared Millimeter Waves* **17**, 1997 (1996).

¹²W. W. Ho, *Millimeter-wave Dielectric Properties of Infrared Window Materials*, Infrared Systems and Components, SPIE Vol. 750 (SPIE, 1987), p. 161.

¹³D. Harris, *Infrared Window and Dome Materials, Tutorial Texts in Optical Engineering*, SPIE Vol. TT10 (SPIE, 1992), pp. 46–47 (Table 1.7, Fig. 140).